

## Arginine-Rich Molecular Transporters for Drug Delivery: Role of Backbone Spacing in Cellular Uptake

Jonathan B. Rothbard,<sup>†</sup> Erik Kreider,<sup>†</sup> Christopher L. VanDeusen,<sup>‡</sup> Lee Wright,<sup>†</sup> Bryan L. Wylie,<sup>†</sup> and Paul A. Wender<sup>\*,‡</sup>

CellGate Inc., 552 Del Rey Avenue, Sunnyvale, California 94085, and Department of Chemistry, Stanford University, Stanford, California 95304

Received December 13, 2001

Short oligomers of arginine, either alone or when conjugated to therapeutic agents or large biopolymers, have been shown to cross readily a variety of biological barriers (e.g., lipid bilayers and epithelial tissue). Molecular modeling suggests that only a subset of the side chain guanidinium groups of these transporters might be required for transport involving contact with a common surface such as a plasma membrane or cell surface receptor. To evaluate this hypothesis, a series of decamers were prepared that incorporated seven arginines and three nonarginine residues. Several of these mixed decamers were comparable to the all arginine decamer in their ability to enter cells. More significantly, these decamers containing seven arginines performed almost without exception better than heptaarginine itself, suggesting that spacing between residues is also important for transport. The influence of spacing was more fully evaluated with a library of oligomers incorporating seven arginines separated by one or more nonconsecutive, non- $\alpha$ -amino acids. This study led to the identification of a new series of highly efficient molecular transporters.

### Introduction

Biological barriers have evolved to prevent entry of xenobiotics into tissues and cells. However, these same barriers often limit or preclude uptake, and therefore the therapeutic benefit, of a variety of drugs.<sup>1</sup> Consequently, most drugs must be restricted in physical properties to allow passage through the polar extracellular milieu and passive diffusion through the relatively nonpolar bilayer of a cell. These opposing polarity preferences limit the universe of potential therapeutics to a very small number of compounds. The studies described herein were directed toward the goal of enhancing or enabling the delivery of drugs through biological barriers by conjugation to transporter molecules that enhance both water solubility and cellular uptake.<sup>2–6</sup>

In the past several years, a variety of peptides, many of which were present in viral proteins, were shown to be capable of crossing biological membranes of a variety of cell types.<sup>7</sup> Previous studies have established that the biological activity of a subgroup of such peptide transporters arose from their high arginine content.<sup>8,9</sup> Oligomers of arginine composed of six or more amino acids, either alone or when covalently attached to a variety of small molecules, cross biological membranes very efficiently by a currently undefined mechanism that is temperature sensitive, but is still efficient at 4 °C, and is inhibited by pretreatment with sodium azide.<sup>8,9</sup> The guanidinium headgroups of the arginines are critical for transport, while the chirality of the amino acid, the length of the side chain, and the spacing and composition of the backbone can be varied.<sup>8,10</sup> The rate of uptake

is dependent on both the concentration of the oligomers and the guanidine content, with increased rate observed as the length of the peptide is increased to approximately 15 residues. Longer oligomers enter cells effectively but also precipitate serum proteins and exhibit cellular cytotoxicity at high micromolar concentrations. Detailed kinetic analyses of nonamers of arginine indicate that they are significantly more effective at crossing biological membranes than the nonapeptide of tat, residues 49–57, and the 16 amino acid peptide from antennapedia.<sup>10</sup> Interestingly, the activity of the tat peptide, which contains six arginines, is comparable to a hexamer of arginine.<sup>10</sup>

Even though oligomers of D- and L-arginine enter cells equally well in vitro in the absence of serum, they differ significantly in their biological effects. Intracellular proteolysis of oligomers of L-arginine effectively provides L-arginine as a substrate for induced nitric oxide synthase (i-NOS) in vascular smooth muscle endothelial cells, which has been shown to be therapeutically useful in animal models of venous–arterial grafts and transplantation.<sup>11–13</sup>

The importance of the guanidinium headgroup in transport is supported by the observation that short oligomers of arginine entered cells far more rapidly than the corresponding oligomers of either lysine, histidine, ornithine, or citrulline.<sup>8</sup> Additional support was gained from examining the ability of a family of polyguanidine peptoids that differed in the length and flexibility of their side chains.<sup>10</sup> Importantly, the ability of these peptoids to enter cells improved when the length of the side chain, and consequently their conformational freedom, increased. This result suggested that increasing the flexibility of the side chains might allow a higher percentage of guanidines to contact simultaneously a biological membrane or receptor.

\* To whom correspondence should be addressed. Tel: (650)723-0208. Fax: (650)725-0259. E-mail: wenderp@stanford.edu.

<sup>†</sup> CellGate Inc..

<sup>‡</sup> Stanford University.

**Table 1.** All Possible Permutations of the Insertion of between One and Six Aminocaproic Acids (aca) into a Heptamer of Arginine<sup>a</sup>

	code		code		code		code	
1	0	RRRRRRR	23	3.1	RacaRacaRacaRRRR	44	4.2	RacaRacaRacaRRacaRR
2	1.1	RacaRRRRRRR	24	3.2	RacaRacaRRacaRRR	45	4.3	RacaRacaRacaRRRacaR
3	1.2	RRacaRRRRR	25	3.3	RacaRacaRRRacaRR	46	4.4	RacaRacaRRacaRacaRR
4	1.3	RRRacaRRRR	26	3.4	RacaRacaRRRacaR	47	4.5	RacaRacaRRacaRRacaR
5	1.4	RRRRacaRRR	27	3.5	RacaRRacaRacaRRR	48	4.6	RacaRacaRRRacaRacaR
6	1.5	RRRRRacaRR	28	3.6	RacaRRacaRRacaRR	49	4.7	RacaRRacaRacaRacaRR
7	1.6	RRRRRRacaR	29	3.7	RacaRRacaRRRacaR	50	4.8	RacaRRacaRacaRRacaR
8	2.1	RacaRacaRRRRR	30	3.8	RacaRRRacaRacaRR	51	4.9	RacaRRacaRRacaRacaR
9	2.2	RacaRRacaRRRR	31	3.9	RacaRRRacaRRacaR	52	4.10	RacaRRRacaRacaRacaR
10	2.3	RacaRRRacaRRR	32	3.10	RacaRRRacaRacaR	53	4.11	RRacaRacaRacaRacaRR
11	2.4	RacaRRRRacaRR	33	3.11	RRacaRacaRacaRRR	54	4.12	RRacaRacaRacaRRacaR
12	2.5	RacaRRRRRacaR	34	3.12	RRacaRacaRRacaRR	55	4.13	RRacaRacaRRacaRacaR
13	2.6	RRacaRacaRRRR	35	3.13	RRacaRacaRRRacaR	56	4.14	RRacaRRacaRacaRacaR
14	2.7	RRacaRRacaRRR	36	3.14	RRacaRRacaRacaRR	57	4.15	RRacaRacaRacaRacaR
15	2.8	RRacaRRRacaRR	37	3.15	RRacaRRacaRRacaR	58	5.1	RacaRacaRacaRacaRacaRR
16	2.9	RRacaRRRRacaR	38	3.16	RRacaRRRacaRacaR	59	5.2	RacaRacaRacaRacaRRacaR
17	2.10	RRRacaRacaRRR	39	3.18	RRRacaRacaRacaRR	60	5.3	RacaRacaRacaRRacaRacaR
18	2.11	RRRacaRRacaRR	40	3.19	RRRacaRacaRRacaR	61	5.4	RacaRacaRRacaRacaRacaR
19	2.12	RRRacaRRRacaR	41	3.20	RRRacaRRacaRacaR	62	5.5	RacaRacaRacaRacaRacaR
20	2.13	RRRRacaRacaRR	42	3.21	RRRRacaRacaRacaR	63	5.6	RRacaRacaRacaRacaRacaR
21	2.14	RRRRacaRRacaR	43	4.1	RacaRacaRacaRacaRRR	64	6.1	RacaRacaRacaRacaRacaR
22	2.15	RRRRRacaRacaR						

<sup>a</sup> The individual peptides are referred to using the codes that also include the number of substitutions in their format.

To determine the spatial preferences of the guanidinium headgroups in a decamer of L-arginine, the peptide was modeled by computer to identify families of low energy conformers. In one preferred family of conformers, seven of the 10 guanidinium groups displayed directionality that was opposite to the other three side chains (at the 2nd, 5th, and 8th residues). In this conformer family, the latter residues did not appear to be capable of contributing to the formation of a complex with a common surface. Uptake is of course a dynamic process, but this modeling suggests that at any one time point in the uptake process only a subset of the arginines residues directly contribute. To explore this possibility, the 2nd, 5th, and 8th residues of a decamer were substituted in turn with each of the naturally occurring  $\alpha$ -amino acids. As suggested by modeling, several of these decamers containing only seven arginines entered cells as well as the unsubstituted decaarginine peptide. More importantly, all but two of the mixed decamers containing seven arginines entered cells more effectively than the corresponding heptaarginine control, suggesting that the spacing between the arginine residues also influences transport. To systematically explore this point, a series of derivatives were synthesized, each containing seven arginines and one or more nonconsecutive non- $\alpha$ -amino acid subunits. The analysis of this set of analogues led to the identification of new molecular transporters that are significantly superior in activity to homopolymers of arginine.

## Experimental Section

**Peptide Synthesis.** Peptides were synthesized using solid phase techniques and commercially available Fmoc amino acids, resins, and reagents (PE Biosystems, Foster City, CA, and Bachem, Torrance, CA) on an Applied Biosystems 433A peptide synthesizer as previously described.<sup>10</sup> Fastmoc cycles were used with O-(7-azabenzotriazol-1-yl)-1, 3, 3-tetramethyluronium hexafluorophosphate (HATU) substituted for HBTU/HOBt as the coupling reagent. All Fmoc amino acids were commercially available (Bachem, San Diego, CA). The peptides were cleaved from the resin using 96% trifluoroacetic acid, 2% triisopropyl silane, and 2% phenol for between 1 and 12 h. The longer reaction times were necessary to completely

remove the Pbf protecting groups from the polymers of arginine. The peptides subsequently were filtered from the resin, precipitated using diethyl ether, purified using high-performance liquid chromatography (HPLC) reverse phase columns (Alltech Altima, Chicago, IL), and characterized using electrospray mass spectrometry (Applied Biosystems, Foster City, CA). Purity of the peptides was shown to be greater than 95% using a PE Biosystems 700E HPLC and a reverse phase column (Alltech Altima).

**Peptide Characterization. Fluorescein aca RRRRRRRRRR CONH<sub>2</sub>.** C<sub>87</sub>H<sub>145</sub>N<sub>43</sub>O<sub>16</sub>S: [M + 5TFA]<sup>5+</sup> = 530.1542 (M = 2080.77, calcd = 2080.1575,  $\Delta$  = 0.6125), [M + 6H]<sup>6+</sup> = 347.7173 (M = 2080.2558, calcd = 2080.1575,  $\Delta$  = 0.0983).

**Fluorescein aca RGRGRGRGRGR CONH<sub>2</sub>.** C<sub>81</sub>H<sub>127</sub>N<sub>37</sub>O<sub>19</sub>S: exact mass, 1953.9830; experimentally observed in ES-TOF: [M + 3H]<sup>3+</sup> = 652.2878 (M = 1953.8634, calcd = 1953.9830,  $\Delta$  = -0.1196), [M + 4H]<sup>4+</sup> = 489.7238 (M = 1954.8952, calcd = 1953.983,  $\Delta$  = 0.9122), [M + 5H]<sup>5+</sup> = 391.7858 (M = 1953.9290, calcd = 1953.9830,  $\Delta$  = -0.054).

**Fluorescein aca R $\beta$ AR $\beta$ AR $\beta$ AR $\beta$ AR $\beta$ AR $\beta$ AR CONH<sub>2</sub>.** C<sub>87</sub>H<sub>139</sub>N<sub>37</sub>O<sub>19</sub>S: exact mass, 2038.0769; experimentally observed in ES-TOF: [M + 5H]<sup>5+</sup> = 408.5912 (M = 2037.9560, calcd = 2038.0769,  $\Delta$  = -0.1209), [M + 6H]<sup>6+</sup> = 340.7115 (M = 2038.269, calcd = 2038.0769,  $\Delta$  = 0.1921).

**Fluorescein aca RabuRabuRabuRabuRabuRabuR CONH<sub>2</sub>.** C<sub>93</sub>H<sub>151</sub>N<sub>37</sub>O<sub>19</sub>S: exact mass, 2122.1708; experimentally observed in ES-TOF: [M + 4H]<sup>4+</sup> = 531.6875 (M = 2122.75, calcd = 2122.1708,  $\Delta$  = 0.5792), [M + 4H]<sup>4+</sup> = 425.5442 (M = 2122.721, calcd = 2122.1708,  $\Delta$  = 0.5502).

**Fluorescein aca RacaRacaRacaRacaRacaRacaR CONH<sub>2</sub>.** C<sub>105</sub>H<sub>175</sub>N<sub>37</sub>O<sub>19</sub>S: exact mass, 2290.3586; experimentally observed in ES-TOF: [M + 4H]<sup>4+</sup> = 573.6652 (M = 2290.6608, calcd = 2290.3586,  $\Delta$  = 0.3022), [M + 5H]<sup>5+</sup> = 459.0128 (M = 2290.064, calcd = 2290.3586,  $\Delta$  = -0.2946).

**Fluorescein aca RaclRaclRaclRaclRaclRaclR CONH<sub>2</sub>.** C<sub>117</sub>H<sub>199</sub>N<sub>37</sub>O<sub>19</sub>S: exact mass, 2458.5464; experimentally observed in ES-TOF: [M + 5H]<sup>5+</sup> = 492.6486 (M = 2458.243, calcd = 2458.5464,  $\Delta$  = -0.3034), [M + 6H]<sup>6+</sup> = 410.6981 (M = 2458.1886, calcd = 2458.5464,  $\Delta$  = -0.3578).

**Robotic Peptide Synthesis.** Parallel solid phase synthesis of the peptides listed in Table 1 was accomplished using an ABI robotics system, the Solaris 450, capable of 48 concurrent syntheses. Identical protected amino acids, resins, and solvents were used in the robotic system as previously described. The peptides were cleaved from the resin using trifluoroacetic acid and purified by reverse phase HPLC, and their structure was

confirmed using electrospray mass spectrometry (Applied Biosystems).

**Molecular Modeling.** NAMD2,<sup>14</sup> developed at the University of Illinois, was used to evaluate the structure of an acetylated decamer of arginine with a carboxamide terminus. The psfgen program was used to create the necessary psf and pdb input files. CHARMM parameters<sup>15</sup> were used to minimize the decamer for 2000 steps using a dielectric constant of 80. At this point, molecular dynamics was performed for 100 ps over which the average kinetic energy of the system was increased from 300 to 1000 K in 25° increments by reassignment every picosecond, holding at 1000 K once reached. Following 20 ps of equilibration, the system was reequilibrated to 300 K over 100 ps in 10° increments every picosecond, holding at 300 K once reached. The annealed structures were then analyzed using VMD.<sup>16</sup>

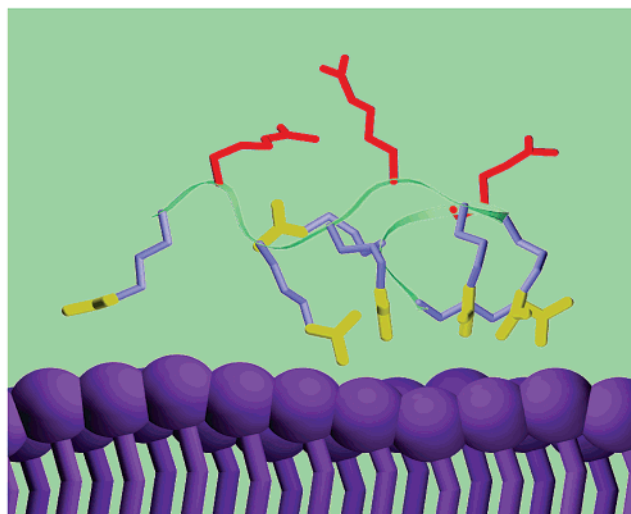
**Cellular Uptake Assays.** The peptides were each dissolved in phosphate-buffered saline (PBS) buffer (pH 7.2), and their concentrations were determined by absorption of fluorescein at 490 nm ( $\epsilon = 67\,000$ ). Weighing selected samples and dissolving them in a known amount of PBS buffer established the accuracy of this method for determining transporter concentration. The concentrations determined by UV spectroscopy correlated with the amounts weighed out manually. The human T cell line, Jurkat, grown in 10% fetal calf serum in Dulbecco's modified Eagles's medium (DMEM), was used for all of the cellular uptake experiments. Varying amounts of the peptides were added to  $3 \times 10^5$  cells in a total of 200  $\mu\text{L}$ , in wells of microtiter plates, and incubated for 3 min at 23 °C. The cells were spun, washed three times with cold PBS, and resuspended in PBS containing 0.1% propidium iodide. The cells were analyzed by fluorescent flow cytometry (FAC-Scan, Becton Dickinson, Milpitas, CA). Cells staining with propidium iodide were excluded from the analysis. Data presented are the mean fluorescent signal for the 5000 cells collected. To prevent cellular uptake of the peptides, the cells were treated with sodium azide (1.0%) for 25 min prior to exposure to the peptides. Intracellular fluorescence was calculated by subtracting the fluorescence from cells treated with sodium azide from that observed from untreated cells.

## Results

This study started with the hypothesis that only a subset of the arginine side chains in a homopolymer would be required for transport across a biological barrier. Computer modeling revealed that for many computer-generated secondary structures of a transporter, the guanidinium headgroups can be grouped by directionality with only a subset of the guanidino groups having a similar orientation as might be required for contact with a cell surface or a protein receptor. While uptake is a dynamic process, this modeling suggests that at any one time point in the process only a subset of the arginines residues might directly contribute. Consequently, the arginines not in contact with the common surface could in principle be replaced with other residues without decreasing transport.

Using NAMD2, a scalable molecular mechanics engine, the solution phase structures of a decamer of arginine were evaluated.<sup>14</sup> One of the low energy conformations found at 300 K had two subsets of guanidine headgroups differing in orientation. One subset consisted of residues 1, 3, 4, 6, 7, 9, and 10 and the second consisted of residues 2, 5, and 8 (Figure 1a). The former set of seven residues shared similar directionality and consequently the potential to contact a common surface such as a membrane or receptor. The latter set of three residues had headgroups with an opposing orientation. Sampling of other conformational families reveals a similar pattern in which only a subset

a.



b.

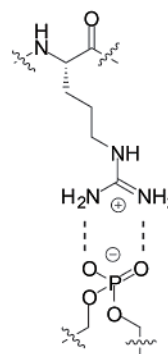


**Figure 1.** Molecular modeling of a low energy conformation of Ac-R10-CONH2 (a) and the chemical structure of the putative bidendate hydrogen-bonding interaction proposed between the guanidine headgroup of arginine and the phosphates present in lipid bilayers (b). The molecular model is displayed as a ribbon structure showing a representative decamer structure with the 2nd, 5th, and 8th side chains in red. A green ribbon represents the backbone of the decamer. The side chains that are able to access a common surface (purple) are shown in blue with guanidinium groups colored yellow.

of the arginine residues in a decamer share a similar directionality. As a starting point for determining whether certain arginine residues could be removed without penalty to transport, a set of 17 decamers possessing arginines at positions 1, 3, 4, 6, 7, 9, and 10 and each of the naturally occurring  $\alpha$ -amino acids, with the exceptions of arginine, cysteine, and tryptophan, at positions 2, 5, and 8 were synthesized, conjugated with fluorescein, and assayed for cellular uptake (Figure 2).

All peptides were decamers containing seven equivalently spaced arginines. These mixed decapeptides exhibited a wide range of abilities to enter the cells due to their differing amino acid substitution at positions 2, 5, and 8. Decapeptides with aspartic and glutamic acids at these positions entered cells relatively poorly. This is in agreement with previous experiments indicating that the guanidine headgroup of arginine can form intramolecular salt bridges with either phosphate or carboxylate functionalities, and in so doing reduce the number of guanidines available for transport (unpublished results). A similar effect could explain the relatively inefficient ability of the peptides substituted with



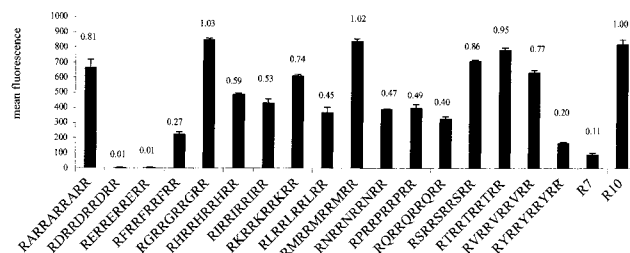


**Figure 2.** Differential cellular uptake of a set of decamers with each of the naturally occurring amino acids substituted in positions 2, 5, and 8 as compared with R7 and R10. The mean fluorescence from 5000 cells of a human T cell line, Jurkat, is shown after incubation with 25  $\mu$ M of each of the peptides for 5 min. Uptake was measured in triplicate at concentrations varying from 400 nM to 50  $\mu$ M. The uptake relative to R10 is quantified above each bar. The data are shown at a single concentration for ease of presentation. The details of the assay are described in the Experimental Section.

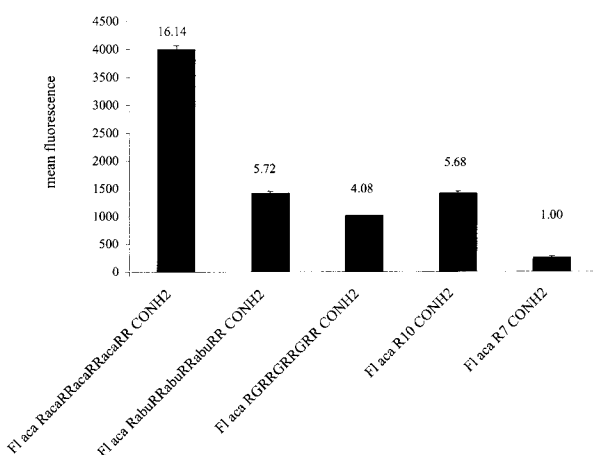


**Figure 3.** Relative ability of a set of decamer analogues with substitution at residues 2, 5, and 8 resulting in differential spacing between the arginines. The mean fluorescence from 5000 cells of a human T cell line, Jurkat, is shown after incubation with 12.5  $\mu$ M of each of the peptides for 5 min. Uptake was measured in triplicate at concentrations varying from 400 nM to 50  $\mu$ M. The data are shown at a single concentration for ease of presentation. The numbers above the histograms represent the relative uptake as compared to hepta L-arginine, R7.

the acidic amino acids to enter cells. Importantly, substitution at positions 2, 5, and 8 with valine, alanine, glycine, methionine, and threonine resulted in analogues that entered cells as well as R10, even though they each contained only seven guanidino groups. This supported the initial hypothesis that only a subset of the guanidine headgroups is necessary for efficient cellular uptake.

Another factor contributing to transport activity is revealed when the peptides containing seven arginines and three variable residues are compared with R7 (Figure 3). With the exception of the acidic amino acid substitutions, all of these decapeptides containing seven arginines were superior to R7, suggesting that an increase in the spacing between the arginine residues also enhances cellular uptake.

To explore this point further, two decamers of arginine were synthesized; one with 4-aminobutyric acid (abu) and the other with 6-aminocaproic acid (aca) substituted for arginine at residues 2, 5, and 8. Their ability to enter lymphocytes was compared with the

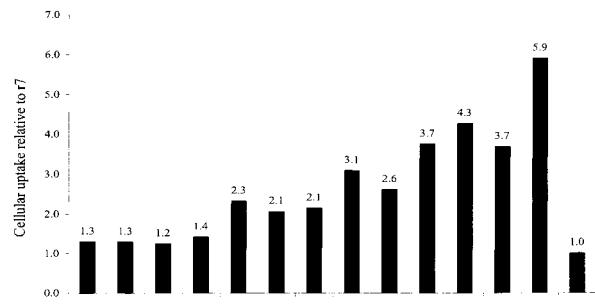


**Figure 4.** Differential uptake of heptamers of L-arginine with varying numbers of aminocaproic acid interspersed into the sequence. Codes refer to peptides listed in Table 1. Each peptide was assayed from 400 nM to 50  $\mu$ M, but only the differential uptake at 12.5  $\mu$ M is shown. The data above the bars are presented as relative uptake as compared to hepta D-arginine, r7.

glycine-substituted analogue and the two homopolymers, R7 and R10 (Figure 3). The differential uptake of the peptides supported the view that increasing the spacing between the arginines would result in greater cellular uptake. Glycine has a single methylene between the amino and the carboxyl groups, 4-aminobutyric acid has three, and 6-aminocaproic acid has five. As the number of methylenes increased from one to three to five, the uptake relative to R7 increased by factors of four, five, and 16, respectively. The peptide with aminocaproic acid spacing entered cells more effectively than R10.

The data in Figure 3 established that the spacing between the arginine residues was an important factor in the structure–activity relationship of cellular uptake. However, only a single substitution pattern was examined. The dynamics of the uptake process suggest that other patterns could be important. There are actually 63 unique sequences in which seven arginines are spaced by 1–6 nonconsecutive 1,6-aminocaproic acids (Table 1). When these aca-spaced peptides were assayed for cellular uptake, a relatively simple pattern was observed. The rate of uptake is dependent on the aminocaproic acid content, and the individual pattern of spacing is unimportant. Peptides with greater aminocaproic acid content exhibit faster rates of uptake. Peptides with equal numbers of aminocaproic acids located differently within the sequence enter cells comparably well (Figure 4 and data not shown). The most potent analogue is the fully spaced compound, analogue 6.1, which has six aminocaproic acids, one between each of the seven arginines (Figure 4).

Such a simple pattern is consistent with the importance of either a flexible association with a receptor for turnover or the association with negatively charged species on the cell surface as required for internalization. An alternative explanation of the data is that as more aminocaproic acids were introduced into the heptamer of arginine the peptide became more protease resistant. Consequently, the peptides containing more aminocaproic acids would have a higher effective concentration. Even though only a trace amount of serum was in the assay, this possibility cannot be eliminated at this time.

To attempt to distinguish between these possibilities and also to determine the optimal linear spacer, the set

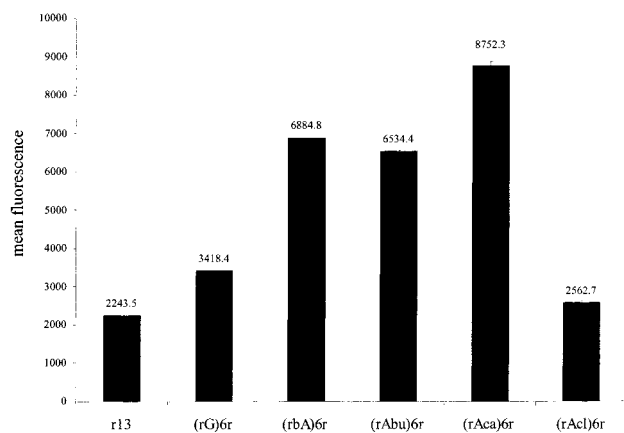


**Figure 5.** Cellular uptake increased as the spacing between the arginines increased until the residues were separated by 8-aminocaproic acid. Comparison of the cellular uptake of a set of peptides containing seven arginine and either six alternating glycine ( $\text{CH}_2=1$ ),  $\beta$ -alanine ( $\text{CH}_2=2$ ), 4-aminobutyric acid ( $\text{CH}_2=3$ ), 6-amino caproic acid ( $\text{CH}_2=5$ ), or 8-aminocaproic acid ( $\text{CH}_2=7$ ) with both r13. The mean fluorescence from 5000 cells of a human T cell line, Jurkat, is shown after incubation with  $12.5 \mu\text{M}$  of each of the peptides for 5 min. Uptake was measured in triplicate at concentrations varying from  $400 \text{ nM}$  to  $50 \mu\text{M}$ . The data are shown at a single concentration for ease of presentation.

of peptides containing seven arginines with either six alternating glycine ( $\text{CH}_2=1$ ),  $\beta$ -alanine ( $\text{CH}_2=2$ ), 4-aminobutyric acid ( $\text{CH}_2=3$ ), 6-amino caproic acid ( $\text{CH}_2=5$ ), or 8-aminocaproic acid ( $\text{CH}_2=7$ ) residues were synthesized and assayed for cellular uptake (Figure 5). In this set of peptides, D-arginine was incorporated to eliminate the possibility of differential proteolysis affecting the results. With the exception of the peptide containing  $\beta$ -alanine being superior to that containing 4-amino butyric acid, a general trend was observed in which an increased rate of uptake into cells correlated with increased spacing between the arginines, until a limit was reached with the 6-aminocaproic acid.

A characteristic of arginine rich transporters is that their ability to enter cells correlates with their arginine content. To test whether the spaced peptides share this characteristic, a set of spaced peptides with an arginine content ranging from five to seven were synthesized and assayed (Figure 6). Among a family of peptides with the arginine residues equally spaced, increasing the arginine content increased the rate of cellular uptake.

## Discussion

The fundamental goal of this research was to determine the structural requirements for cellular uptake of guanidine rich transporters and to use this information to develop more effective molecular transporters. The importance of the guanidino headgroup and the apparent insensitivity to the oligomer's chirality were revealed in our initial peptide studies. Subsequently, a series of novel polyguanidine peptoids incorporating the arginine side chain were prepared and found to exhibit comparable cellular uptake to the corresponding D-arginine peptides r5, r7, and r9, indicating that the hydrogen bonding along the peptide backbone and backbone chirality was not essential for cellular uptake. This observation was consistent with molecular models of these peptoids, arginine oligomers, and Tat<sub>49-57</sub>, all

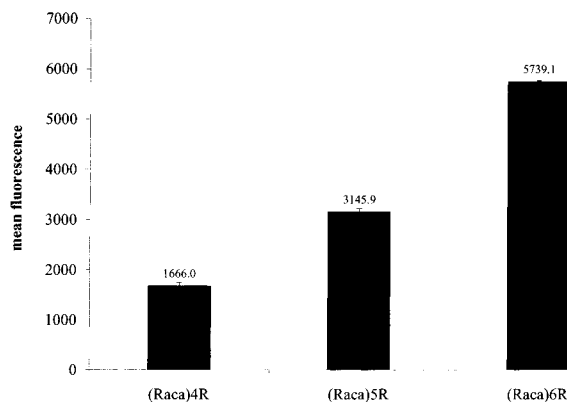


**Figure 6.** Peptides with greater arginine content exhibit faster rates of cellular uptake. Comparison of the cellular uptake of fluorescent peptides composed of five, six, or seven arginines interspaced with 6-aminocaproic acid residues. Uptake was measured in triplicate at concentrations varying from  $400 \text{ nM}$  to  $50 \mu\text{M}$ , but only the differential uptake at  $12.5 \mu\text{M}$  is shown.

of which have a deeply embedded backbone and a guanidinium-dominated surface.

To determine whether all, or only a subset, of the headgroups in an oligomer were necessary for optimal activity, computer modeling of the arginine decamer was done. The modeling revealed conformations in which subsets of the guanidinium groups shared directionality as might be required to contact a common surface. In one low energy family of conformers, seven of the 10 guanidinium groups had a similar orientation. A series of derivatives that retained these seven residues but which incorporated various  $\alpha$ -amino acid residues at the remaining three positions were synthesized and evaluated for uptake. The data shown in Figure 2 demonstrate that several decamers consisting of seven arginines and various amino acids at positions 2, 5, and 8 performed as well as the unsubstituted decamer of arginine. These data support the hypothesis that only a subset of the headgroups in the peptide transporter is necessary for efficient uptake.

Significantly, with the exception of the analogues containing substitutions with aspartic and glutamic acid, all of the decamers containing seven arginines were more efficient in uptake than heptaarginine itself. These data indicate that independent of the characteristics of the side chain, an increase in spacing between the arginine residues also leads to an increase in cellular uptake. This improved performance was further enhanced when non- $\alpha$ -amino acids were substituted into the 2nd, 5th, and 8th positions. The rate of uptake increased as the number of methylenes in the non- $\alpha$ -amino acids increased.

This substitution pattern was only one of 63 different possible permutations of nonconsecutive spacer residues that could be inserted into a heptamer of arginine. To determine the optimal spacing pattern for substituting up to six nonconsecutive 6-aminocaproic acids into a heptamer of arginine, a series of substituted peptides were synthesized in parallel and then assayed for cellular uptake. A simple pattern was observed. Greater cellular uptake was observed as the number of aca units in the analogue increased. The exact location was unimportant, in that all analogues with a single aminocaproic acid were approximately equivalent and less

effective than those with two amino acid spacers. Increased cellular uptake was seen as more aminocaproic acid residues were added, until reaching the fully substituted analogue containing six spacer amino acids, one between each of the seven arginines.

These data do not differentiate between improved uptake and suppression of metabolism. Peptides containing greater aminocaproic acid content would be more resistant to proteolysis and thereby would be expected to increase the effective half-life of the more highly substituted analogues. Alternatively, the increased distance between the arginine residues can result in superior cellular uptake. Support for the latter hypothesis arises from the observation that a set of peptides containing seven D-arginines with either alternating glycine ( $\text{CH}_2=1$ ),  $\beta$ -alanine ( $\text{CH}_2=2$ ), 4-amino butyric acid ( $\text{CH}_2=3$ ), 6-amino caproic acid ( $\text{CH}_2=5$ ), or 8-aminocaprylic acid ( $\text{CH}_2=7$ ) differentially entered cells. Uptake increased as the spacing between the arginines increased from  $\text{CH}_2=1$  until  $\text{CH}_2=5$ , with the exception that the  $\beta$ -alanine-substituted peptide was slightly superior to the one containing 4-amino butyric acid. The trend had limits, as the analogue with 8-amino caprylic acid was less potent than the one containing aminocaproic acid.

The enhanced uptake when non- $\alpha$ -amino acids were substituted into the peptide backbone was very similar to the effect observed when the side chains were extended in the peptoid series.<sup>10</sup> By increasing the conformational freedom of the backbone of peptides through the addition of methylene units, a significant enhancement in the rate of cellular uptake of the transporter was seen. Even though the structural basis for the conformational flexibility of peptoids and peptides is very different, addition of methylenes in either the backbone or the side chain results in enhanced cellular uptake.

The biological activity of most ligands, particularly those functioning as inhibitors, increases with conformational restriction as preorganization in the form of the bound conformer favors tighter binding. The enhanced activity associated with increased conformational mobility observed for molecular transporters is in agreement with a dynamic transport system in which turnover rather than tightness of binding is critical for function. These results combined with earlier studies<sup>8</sup> demonstrating a lack of chiral recognition emphasize the importance of flexible association.

In addition to a receptor-mediated pathway, the transporters could be forming ionic complexes with negatively charged entities on the surface of the biological membranes, such as the phosphates of phospholipids (Figure 1b). The neutralization of the phosphate headgroups of lipids with polycations has been shown to have manifold effects due to the neutralization of the charge, ranging from disruption of the order of the bilayer to release of the associated membrane proteins into the media.<sup>17</sup> Such an interaction certainly would allow two otherwise polar entities to form a relatively nonpolar aggregate capable of moving through a cell bilayer. In this mechanistic model, flexibility along with reach are important as a transporter would need to associate with an ensemble of complementary charged functionalities while minimizing an entropy cost.

The increased flexibility of the transporter might result in greater efficacy by allowing the molecule to adopt significantly different conformations that are necessary for the different steps in translocation. This possibility is consistent with the study demonstrating that a single, common secondary structure induced by model membrane systems was not observed for three transport peptides based on the antennapedia sequence.<sup>18</sup> Alternatively, the peptide might need to adopt a single conformation for biological activity, as is the case for amphipathic, antimicrobial peptides.<sup>19,20</sup> Increased flexibility in the backbone or in the side chains could allow the guanidine headgroups to interact more effectively with negative charges on the cell surface. Using CPK models, increasing the number of methylenes between the arginines not only allows them to interact with negative charges further apart than in homopolymers of arginine but also, interestingly, permits the guanidines to pack more closely and interact with putative negative charges that are closely spaced. Further experiments to distinguish between these possible mechanisms are in progress.

**Acknowledgment.** Support of this work by grants (P.A.W.) from the National Institutes of Health (CA31841, CA31845) and a Stanford Graduate Fellowship (C.L.V.D.) is gratefully acknowledged.

## References

- (1) Lebleu, B. Delivering information-rich drugs—prospects and challenges. *Trends Biotechnol.* **1996**, *14*, 109–110.
- (2) Frankel, A. D.; Pabo, C. O. Cellular uptake of the tat protein from human immunodeficiency virus. *Cell* **1988**, *55*, 1189–1193.
- (3) Derossi, D.; Joliet, A. H.; Chassaing, G.; Prochiantz, A. The third helix of the Antennapedia homeodomain translocates through biological membranes. *J. Biol. Chem.* **1994**, *269*, 10444–10450.
- (4) Schwarze, S. R.; Ho, A.; Vocero-Akbani, A.; Dowdy, S. F. In vivo protein transduction: delivery of a biologically active protein into the mouse [see comments]. *Science* **1999**, *285*, 1569–1572.
- (5) Schwartz, J. J.; Zhang, S. Peptide-mediated cellular delivery. *Curr. Opin. Mol. Ther.* **2000**, *2*, 162–167.
- (6) Rothbard, J. B.; Garlington, S.; Lin, Q.; Kirschberg, T.; Kreider, E.; et al. Conjugation of arginine oligomers to cyclosporin A facilitates topical delivery and inhibition of inflammation. *Nat. Med.* **2000**, *6*, 1253–1257.
- (7) Fischer, P. M.; Krausz, E.; Lane, D. P. Cellular delivery of impermeable effector molecules in the form of conjugates with peptides capable of mediating membrane translocation. *Bioconjugate Chem.* **2001**, *12*, 825–841.
- (8) Mitchell, D. J.; Kim, D. T.; Steinman, L.; Fathman, C. G.; Rothbard, J. B. Polyarginine enters cells more efficiently than other polycationic homopolymers. *J. Pept. Res.* **2000**, *56*, 318–325.
- (9) Futaki, S.; Suzuki, T.; Ohashi, W.; Yagami, T.; Tanaka, S.; et al. Arginine-rich peptides. An abundant source of membrane-permeable peptides having potential as carriers for intracellular protein delivery. *J. Biol. Chem.* **2001**, *276*, 5836–5840.
- (10) Wender, P. A.; Mitchell, D. J.; Pattabiraman, K.; Pelkey, E. T.; Steinman, L.; et al. The design, synthesis, and evaluation of molecules that enable or enhance cellular uptake: peptoid molecular transporters. *Proc. Natl. Acad. Sci. U.S.A.* **2000**, *97*, 13003–13008.
- (11) Uemura, S.; Fathman, C. G.; Rothbard, J. B.; Cooke, J. P. Rapid and efficient vascular transport of arginine polymers inhibits myointimal hyperplasia. *Circulation* **2000**, *102*, 2629–2635.
- (12) Kown, M. H.; Yamaguchi, A.; Jahncke, C. L.; Miniati, D.; Murata, S.; et al. L-arginine polymers inhibit the development of vein graft neointimal hyperplasia. *J. Thorac. Cardiovasc. Surg.* **2001**, *121*, 971–980.
- (13) Kown, M. H.; van Der Steenhoven, T.; Uemura, S.; Jahncke, C. L.; Hoyt, G. E.; et al. L-arginine polymer mediated inhibition of graft coronary artery disease after cardiac transplantation. *Transplantation* **2001**, *71*, 1542–1548.
- (14) Kale, L.; Skeel, R.; Bhandarkar, M.; Brunner, R.; Gursoy, A.; et al. NAMD2: Greater scalability for parallel molecular dynamics. *J. Comput. Phys.* **1999**, *151*, 283–312.

- (15) MacKerell, A. D.; Bashford, D.; Bellott, M.; Dunbrack, R. L.; Evanseck, J. D.; et al. All atom empirical potential for molecular modeling and dynamics studies of proteins. *J. Phys. Chem.* **1998**, *102*, 3586–3616.
- (16) Humphrey, W.; Dalke, A.; Schulten, K. VMD-Visual Molecular Dynamics. *J. Mol. Graph.* **1996**, *14*, 33–38.
- (17) Bellet-Amalric, E.; Blaudez, D.; Desbat, B.; Graner, F.; Gauthier, F.; et al. Interaction of the third helix of Antennapedia homeodomain and a phospholipid monolayer, studied by ellipsometry and PM-IRRAS at the air–water interface. *Biochim. Biophys. Acta* **2000**, *1467*, 131–143.
- (18) Magzoub, M.; Kilk, K.; Eriksson, L. E.; Langel, U.; Graslund, A. Interaction and structure induction of cell-penetrating peptides in the presence of phospholipid vesicles. *Biochim. Biophys. Acta* **2001**, *1512*, 77–89.
- (19) Dathe, M.; Wieprecht, T. Structural features of helical antimicrobial peptides: their potential to modulate activity on model membranes and biological cells. *Biochim. Biophys. Acta* **1999**, *1462*, 71–87.
- (20) Shai, Y. Mechanism of the binding, insertion and destabilization of phospholipid bilayer membranes by alpha-helical antimicrobial and cell nonselective membrane-lytic peptides. *Biochim. Biophys. Acta* **1999**, *1462*, 55–70.

JM0105676